

# Photophysical and photochemical characterisation of bacterial semiconductor cadmium sulfide particles

Peter R. Smith,<sup>a</sup> Justin D. Holmes,<sup>a</sup> David J. Richardson,<sup>b</sup> David A. Russell<sup>a</sup> and John R. Sodeau<sup>a\*</sup>

<sup>a</sup> School of Chemical Sciences and <sup>b</sup> School of Biological Sciences, University of East Anglia, Norwich, UK NR4 7TJ

*Klebsiella pneumoniae* forms electron-dense cadmium sulfide particles (ca. 5–200 nm in diameter) on the cell surface in response to the presence of cadmium ions in the growth medium. In the current study, these ‘bio-semiconductor’ particles have been spectroscopically characterised using UV–VIS absorption and luminescence analysis. The spectroscopic properties observed suggest that they are similar in size and possess photoactive traits analogous to CdS systems prepared by conventional chemical methods. The optical nature of the bacterial semiconductor particles means that, in principle, they are capable of performing a variety of photoredox reactions. The reactions involving photoelectrochemical indicators such as methyl viologen (MV<sup>2+</sup>) and methyl orange (MO<sup>-</sup>) are considered and, by comparing initial rates of reaction and altering reaction variables, a general mechanism of photoactivity for the cadmium sulfide ‘bio-semiconductor’ is proposed.

The bacterium *Klebsiella pneumoniae* is able to transform cadmium ions into nanometer-sized cadmium sulfide particles which are deposited onto the cell surface. Such a biosynthetic mechanism overcomes the toxic effect of any cadmium species, which may be present in the bacterium’s local environment. Aspects of this biochemical process have been reported in the literature, including the kinetics of particle formation and their growth characteristics.<sup>1–5</sup> It was concluded from previous results that the large ‘superparticles’ observed by electron microscopy (EM), e.g. 200 nm, were actually built up from smaller particle aggregates ca. 4 nm in diameter.<sup>5</sup> In conventional chemical studies these small dimension species are termed ‘Q-particles’ and have been shown to possess distinctive photochemical and photophysical properties. Therefore the main aim of the present investigation was to compare and contrast the electronic and photoredox properties of the bio-particles with their well studied chemical counterparts.

There have been many reports in the literature relating to the photoprocesses associated with colloidal semiconductor systems.<sup>6–9</sup> The majority are related to particles produced and supported within chemically synthesised environments, e.g. microemulsions, but few such investigations of biologically generated semiconductor particles have been reported.<sup>10–13</sup> One of the earliest reports was centred on the electronic spectroscopy associated with CdS ‘peptide-capped’ intracellular particles formed within the yeasts *Candida glabrata* and *Schizosaccharomyces pombe*.<sup>11–18</sup>

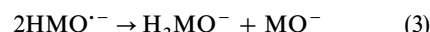
Recently some of the key photobiological and spectroscopic features associated with the *K. pneumoniae* system have been published. For example, CdS bio-particles have been shown to photoprotect the bacterium from destructive UV-A radiation ( $\lambda = 320\text{--}400\text{ nm}$ )<sup>2</sup> and to produce both oxygen- and carbon-based radicals upon illumination with visible light.<sup>19</sup> Furthermore it has been established that the onset of absorption ( $\lambda_{\text{onset}}$ ) for the extracellular bio-particles of CdS lies in the wavelength range between 440–450 nm with an absorption maximum wavelength ( $\lambda_{\text{max}}$ ) between 400 and 410 nm.<sup>2,5,19</sup> This absorption profile corresponds to a particle size of ca. 4 nm from a Henglein plot and an energy band gap of 2.9–3.25 eV.<sup>20,21</sup> Preliminary accounts of CdS bio-particle photoredox properties have also been given and this behaviour is discussed in some detail within this report because of the potential applications in light-driven electron-transfer reactions.<sup>19</sup>

The photochemistry of bipyridinium salts, such as methyl viologen (MV<sup>2+</sup>) and methyl orange (MO<sup>-</sup>) are well documented.<sup>22–30</sup> The reduced forms of both MV<sup>2+</sup> and MO<sup>-</sup> display strong absorption bands in the visible region of the spectrum, making them easy to monitor in any investigation of their photoredox chemistry. In fact, the viologens exist in three main oxidation states,<sup>24,25</sup> namely  $\text{V}^{2+} \rightleftharpoons \text{V}^{\cdot+} \rightleftharpoons \text{V}^0$ .

The effects of irradiating chemically synthesised CdS colloidal systems in the presence of MV<sup>2+</sup> and MO<sup>-</sup> have also been previously reported.<sup>20,31</sup> The reduction of MV<sup>2+</sup> ions to MV<sup>\cdot+</sup> radical ions can be monitored from the electronic absorption spectrum as the radical cation is blue with absorption bands at  $\lambda$  ca. 600 and 465 nm.

In some cases it has been reported that the MV<sup>\cdot+</sup> radical ion can re-form the parent MV<sup>2+</sup> by passing an electron to another acceptor: this process is termed ‘electron relay’. For example, in mixed systems of methyl viologen and methyl orange with colloidal CdS an unexpected enhancement of MO<sup>-</sup> reduction can be explained in terms of this effect.<sup>29,30</sup>

The kinetics of methyl orange reduction photosensitised by colloidal CdS have also been well documented.<sup>27–29</sup> The rate determining step has been established as the reduction of the unprotonated form of the MO<sup>-</sup> to the semi-reduced radical HMO<sup>\cdot-</sup> via reaction (1):<sup>27,28</sup>



The subsequent reactions which lead to hydrazine formation [reactions (2) and (3)] are much faster than reaction (1). MO<sup>-</sup> has an absorption maximum at  $\lambda_{\text{max}} = 463\text{ nm}$ , whereas the secondary hydrazine derivative is colourless ( $\lambda_{\text{max}} = 247\text{ nm}$ ). It is these absorption characteristics that lead to the use of methyl orange as a probe for photoredox reactions since the reduction of the unprotonated form can be followed by monitoring the decrease in absorbance of the system at a wavelength of 463 nm.<sup>26–29</sup>

In the present study, experiments to determine the CdS bio-particles’ luminescence and to evaluate the extent of their photoredox properties were performed. Contrasts between the photochemical and photophysical behaviour of the bacterial CdS particles compared to their well studied conventional

chemical counterparts should be readily apparent. Several key factors such as the effect of pH on the reduction rates of the positively charged viologen,  $MV^{2+}$  and the negatively charged  $MO^-$  were monitored.

## Experimental

### Growth of bacterium and formation of CdS crystallites

The Class II pathogen *Klebsiella pneumoniae* (previously known as *Klebsiella aerogenes*) NCIMB 418 was used throughout this study. A modification of the growth medium used by Pickett and Dean<sup>32</sup> was used for batch culturing: (contained in 1 l Milli-Q water) 3.2 mg  $FeSO_4 \cdot 7H_2O$ , 64 mg  $MgSO_4 \cdot 7H_2O$ , 0.62 g KCl, 0.60 g sodium  $\beta$ -glycerophosphate and 0.96 g  $(NH_4)_2SO_4$  as the main components in tricine (50 mM) buffered to pH 7.6 using NaOH (2 M). Batch cultures of *K. pneumoniae* were grown under aerobic conditions in sterile conical flasks (250 ml) by inoculating 50 ml of the medium with 100  $\mu$ l *K. pneumoniae* stock suspension in the absence of cadmium ions ('unloaded'). To produce the samples containing 'bio-CdS' particles on the bacterial surface ('loaded'), cadmium ions  $[Cd(NO_3)_2]$  were added at a concentration of 1 mM and the flasks were then shaken for 24 h at 310 K. At the time of inoculation the approximate cell density was  $10^6$  cells  $ml^{-1}$ . After 24 h growth the cell density was *ca.*  $10^9$  cells  $ml^{-1}$ . For the loaded samples this corresponded to a CdS concentration of approximately 0.2 mM.<sup>1,5</sup>

### Electronic spectroscopy

UV-VIS absorption measurements were taken of loaded and unloaded bacterial cultures (3 ml, *ca.*  $10^9$  cells  $ml^{-1}$ , 24 h growth), over a pH range 3–12. The appropriate pH was obtained by the addition of either HCl (1 M) or NaOH (1 M) to the bacterial suspension. An Hitachi U-4001 double beam spectrophotometer incorporating a barium sulfate ( $BaSO_4$ ) integrating sphere attachment was used to record the spectra of the loaded samples, referenced against unloaded bacterial samples of the appropriate pH. The integrating sphere collects the scattered light from the turbid samples and redirects it to the detector, hence reducing the loss of light through scattering. Absorption spectra were recorded using 1 cm path-length quartz spectroscopic cuvettes.

Luminescence excitation and emission spectra were recorded for loaded and unloaded bacterial cultures (3 ml, *ca.*  $10^9$  cells  $ml^{-1}$ , 24 h growth), between a pH range 3–12 [obtained by adjustment with either HCl (1 M) or NaOH (1 M)], and over a range of excitation and emission wavelengths. The luminescence characteristics were measured using a Perkin-Elmer LS-50 luminescence spectrometer, with a front surface accessory (FSA) attachment.

### Photoredox reactions

To harvest cells for photoredox studies loaded and unloaded bacterial samples (250 ml) taken from batch cultures (24 h growth) were centrifuged using a Sorval RC-5B Refrigerated Superspeed centrifuge (10000g for 20 min). The supernatant was then removed and the resultant pellet washed in growth medium (minus glucose, 10 ml). This procedure was repeated three times before the pellet was resuspended in the growth medium (minus glucose, 10 ml). For the loaded samples this corresponded to a CdS concentration of *ca.* 4 mM.<sup>1,5</sup> These concentrated bacterial solutions were then sonicated using a Jencons Sonics and Materials Inc. Vibra-Cell (VCX 400W) with a standard horn (13 mm) and replaceable tip for 2 h (amplitude 48%; pulse on 2.5 s, off 1.0 s). The sonicated samples were then diluted, approximately ten-fold ( $[CdS] \approx 0.4$  mM), with growth medium (no glucose) to give an optical density ( $\lambda_{OD} = 650$  nm) of 1.0. These samples (4 ml),

with an initial pH of *ca.* 7, were set to the desired pH using either HCl (2 M) or NaOH (2 M). The individual photoredox species, *i.e.* methyl viologen ( $MV^{2+}$ , 100  $\mu$ M) or methyl orange ( $MO^-$ , 20  $\mu$ M) was added and the sample transferred to a vacuum-line cell attachment.

All photoredox reactions required samples to be degassed thoroughly before illumination to avoid secondary oxidation of the photoredox species by molecular oxygen. Removal of oxygen was achieved by the 'freeze-pump-thaw' method, repeated four times, using a cardice-acetone mixture to freeze the sample with a pressure of 0.1 mbar. The sample was kept under vacuum throughout the experiment and was irradiated, between wavelengths of 350 and 700 nm, with a medium pressure mercury lamp. A water filter cell (10 cm pathlength) was used between the lamp and the sample to remove IR radiation. The reaction was monitored using a Hewlett Packard HP 8452A diode-array spectrophotometer using HP 89532A software, with absorbance measurements taken at wavelengths averaged over a 4 nm range. An absorption reading was recorded every 10 s, with an integration time of 1 s. The data were processed using the 'Calculations' function available on the kinetics software (HP 89532A), allowing best fit treatment to be performed.

Experiments involving methyl viologen (100  $\mu$ M) were monitored at wavelengths of 598, 600 and 602 nm. A high-pass optical filter ( $>515$  nm) was positioned over the entrance slit of the detector to protect it from the high light intensity emitted by the medium pressure mercury lamp. In the case of methyl orange (20  $\mu$ M), the disappearance of the oxidised form which absorbs between  $\lambda = 462$  and 466 nm was monitored. A high-pass optical filter ( $>400$  nm) was used to protect the detector in this instance. Studies of the competitive photoreduction reaction using a composite solution of methyl viologen (100  $\mu$ M) and methyl orange (20  $\mu$ M) were monitored at two wavelengths. The formation of reduced methyl viologen was followed by the absorption at  $\lambda = 600$  nm, and the disappearance of the oxidised form of methyl orange monitored at  $\lambda = 464$  nm. A high-pass filter ( $>400$  nm) was used to protect the detector. All absorbance measurements were referenced against growth medium (no glucose).

## Results and Discussion

### Electronic spectra of extracellular CdS particles

**Absorption spectra.** It has been previously reported that at pH 7 the onset of absorption ( $\lambda_{onset}$ ) for extracellular CdS particles of *K. pneumoniae* lies between the wavelength range 440–450 nm with an absorption maximum wavelength ( $\lambda_{max}$ ) around 400–410 nm.<sup>2,5,19</sup> Therefore as a necessary prelude to an investigation of the effect of pH on the photochemical and photophysical properties of CdS bio-particles, potential modifications to their electronic absorption spectra by pH were monitored.

The absorption profile of samples loaded and unloaded with CdS particles were recorded using a UV-VIS spectrophotometer incorporating an integrating cell attachment. Fig. 1 shows the absorption profiles obtained at pH 3, 7, 10 and 12 for *K. pneumoniae* loaded with CdS particles (using the corresponding unloaded samples as reference).

The profiles clearly show that over a pH range between 3 and 10,  $\lambda_{max}$  lies between 394 and 399 nm. The  $\lambda_{onset}$ , which is obtained by extrapolating the straight line region of the absorption spectrum (between the absorption tail and the shoulder) to the point which intersects the absorption tail, was found to be hypsochromically shifted at low pH values, *e.g.* at pH 3,  $\lambda_{onset} \approx 475$  nm and between pH 7 and 10,  $\lambda_{onset} \approx 440$  nm. Increasing the pH to 12 resulted in an apparent red-shift of  $\lambda_{max}$  by 18–23 nm ( $\lambda_{max} \approx 417$  nm,  $\lambda_{onset} \approx 450$  nm). The intensity of the electronic absorption spectra also appeared to

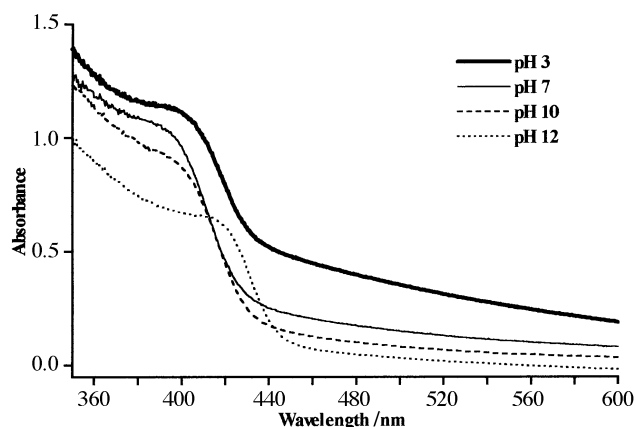


**Fig. 1** Electronic absorption spectra of CdS loaded *K. pneumoniae* cells at various pH values. Spectra recorded using the integrated cell attachment, referenced against unloaded samples.

decrease with increasing pH. This observed intensity effect may, in part, be due to a decrease in the turbidity in the bacterial suspensions as the pH increases. The clarity of the bacterial samples studied was at an optimum for spectroscopic analysis at pH 12. The dependency of the electronic absorption profile on pH was also found to be a reversible process between the pH range 3–12. That is, if the pH of the bacterial solutions were raised and then lowered the absorbance trends remained the same with no permanent change in the absorption spectrum.

**Emission and excitation spectra.** Luminescence studies were performed on *K. pneumoniae* samples loaded and unloaded with cadmium sulfide particles between pH 3–12 and over a range of excitation and emission wavelengths. In all cases a broad feature centred at 350–380 nm was observed: such a band is a typical profile measured for many biological samples and is associated with the luminescence arising from aromatic amino acids in proteins, *e.g.* tyrosine and tryptophan.<sup>33</sup> For both the loaded and unloaded samples, no significant differences were detected between the luminescence emission profiles produced either from excitation at a wavelength ( $\lambda_{\text{ex}}$ ) of 400 nm, *i.e.* the absorption maximum (Fig. 1), at wavelengths above 400 nm, or at pH values below 7. Exciting the loaded and unloaded samples at wavelengths close to  $\lambda_{\text{max}}$  possibly causes biological components present in both sample types to luminesce. This ‘bio-luminescence’ observed in both sample types presumably saturates any signals emanating from the bio-CdS particles. Differences in the emission spectra between the loaded and unloaded samples were only found to occur upon excitation between the wavelength range 250–320 nm and at a pH between 10–12. These results are illustrated in Fig. 2(a) and (b).

At a pH of 12 and a  $\lambda_{\text{ex}} = 270$  nm a luminescence emission wavelength ( $\lambda_{\text{em}}$ ) at  $\approx 450$  nm was observed in the loaded samples, which is close to the onset of absorption of the CdS bio-particles ( $\lambda_{\text{onset}} \approx 450$  nm, pH 12). This luminescence band was absent in the unloaded bacterial samples. By analogy with previous studies on conventional systems, such a feature can be assigned to excitonic luminescence originating from the CdS particles.<sup>31,34</sup> Weak and broad emission bands, commonly observed in inorganic CdS dispersions between wavelengths 500 and 700 nm and attributable to the recombination of charge carriers,<sup>35</sup> were not observed in the loaded CdS samples. Examination of the luminescence excitation spectra for the loaded and unloaded samples revealed that there was little measurable difference between them. Any excitation peaks which could have originated from bio-CdS particles were unresolvable against broad and intense bio-luminescence bands.

For many inorganic CdS particles the intensity of lumines-

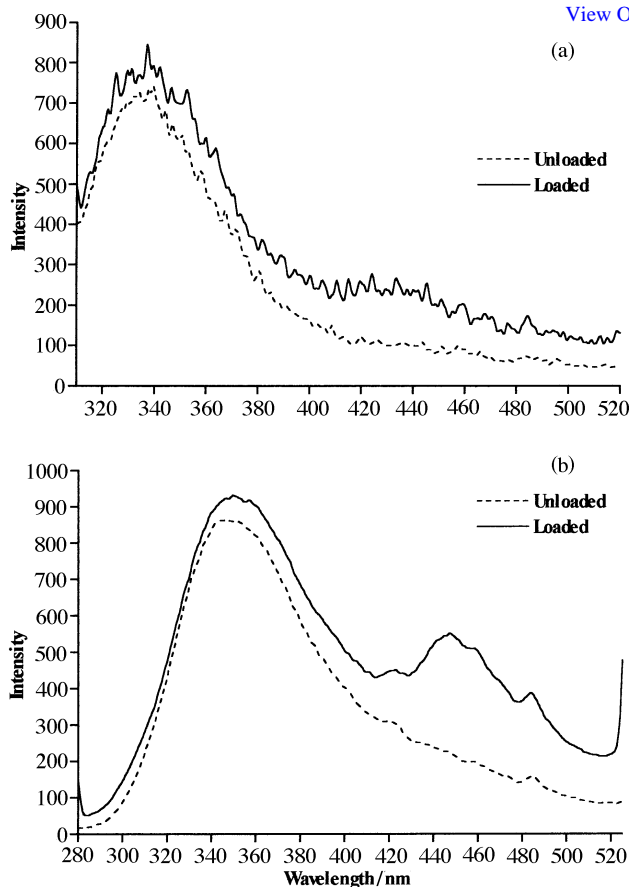


**Fig. 2** (a) Luminescence emission spectra of CdS loaded and unloaded *K. pneumoniae* cells at pH 7,  $\lambda_{\text{ex}} = 270$  nm, slits (excitation : emission) 5.0 : 5.0 nm. (b) Luminescence emission spectra of loaded and unloaded *K. pneumoniae* cells at pH 12,  $\lambda_{\text{ex}} = 270$  nm, slits (excitation : emission) 5.0 : 5.0 nm.

cence is poor but over a period of days subsequent corrosion can increase the luminescence by orders of magnitude. No change in the intensity of luminescence of the bio-CdS particles ( $\lambda_{\text{ex}} = 270$  nm) was noticed over a period of 3–4 weeks. This result therefore suggests that the bio-CdS particles are protected from corrosion, possibly by a biological membrane.<sup>5</sup>

A comparison can be made between the CdS particles formed on *K. pneumoniae* and the ‘peptide-capped’ intracellular particles formed by the yeasts *C. glabrata* and *S. pombe* cultured in the presence of cadmium salts.<sup>11–18</sup> The optical properties of the CdS crystallites formed by these yeasts are size dependent. In *C. glabrata* CdS crystallites 2 nm in diameter, which are stabilised by glutathione ( $\gamma$ -Glu-Cys-Gly) peptides, have been reported by Dameron and Winge<sup>16</sup> to luminesce at a wavelength of 430 nm ( $\lambda_{\text{ex}} = 355$  nm). Acidification of the ‘CdS-yeast’ containing system to pH 1.5 from a pH of 11–13 was shown to be accompanied by a reduction in the luminescence intensity associated with the CdS particles. Such a pH effect was also observed with the loaded samples *K. pneumoniae* investigated in this study. Although there are obvious similarities in the luminescence properties of the two systems, there are also subtle differences in the electronic absorption characteristics. Dameron and Winge<sup>16</sup> have reported that acidification of CdS particles from *C. glabrata* from pH 5 to 4 resulted in an attenuation of  $\lambda_{\text{max}}$  ( $\approx 300$  nm) and a concomitant red shift in  $\lambda_{\text{onset}}$  from 335 nm (pH 5) to 370 nm (pH 4). In contrast they also observed that acidification of CdS particles from *S. pombe* to pH of 4 from a pH of 7–5 led to an attenuation of  $\lambda_{\text{max}}$  ( $\approx 300$  nm) with minimal red-shifting of  $\lambda_{\text{onset}}$ . These observations were not seen in the *K. pneumoniae* CdS system; no attenuation of  $\lambda_{\text{max}}$  occurred upon

acidification and there was a red-shift of  $\lambda_{\text{onset}}$  under basic rather than acid conditions.

The *K. pneumoniae* system is more analogous to the inorganic CdS systems between the pH range 3–10, where the shape of the electronic absorption spectra is unaffected by the pH.<sup>36</sup> It is difficult to postulate if the intensity of absorption of the bio-CdS samples is changing with pH as interferences due to sample turbidity at low pH values obscure the intensities observed. At pH 12 however, unlike with inorganic CdS systems, a hypochromic shift in  $\lambda_{\text{max}}$  was seen. Analogous to the yeast systems mentioned above and the bio-CdS particles investigated in this work, Uchihara *et al.*<sup>36</sup> have reported that the intensity of the luminescence emission profile of both Cd- and S-rich colloids of inorganic CdS increases as the pH increases (particles > 10 nm in diameter,  $\lambda_{\text{ex}} = 355$  nm,  $\lambda_{\text{em}} = 515$  nm). The surface characteristics which might give rise to these observations are discussed in the next section.

### Photoredox reactions

**Methyl viologen.** The luminescence results described above indicate that the photoactivity of the CdS bio-particles is maximised and observable under conditions of high pH. Photolysis experiments using a medium-pressure mercury lamp were therefore performed using loaded and unloaded samples of *K. pneumoniae* at pH 10. Studying the photoredox reactions at pH 10 rather than at a higher pH allows a direct comparison with conventional inorganic CdS systems, also measured at pH 10. Reduction of  $\text{MV}^{2+}$  (100  $\mu\text{M}$ ) was monitored at three wavelengths (598, 600 and 602 nm). The results, shown graphically as absorbance–time plots in Fig. 3, provide evidence that the unloaded samples are not photoactive and that for loaded samples ( $[\text{CdS}] \approx 0.4$  mM) the formation of  $\text{MV}^{+}$  occurs at an initial rate of  $4.8 \times 10^{-9}$  mol dm<sup>-3</sup> s<sup>-1</sup>. This rate is comparable to that obtained using nanocrystalline CdS colloids prepared by Matsumoto *et al.*<sup>22</sup> who report a  $\text{MV}^{+}$  production rate of ca.  $1 \times 10^{-9}$  mol dm<sup>-3</sup> s<sup>-1</sup> by colloidal CdS particles with an average diameter of 4.4 nm, ranging in size from 3 to 8 nm, at pH 10 ( $[\text{CdS}] = 0.06$  mM,  $[\text{MV}^{2+}] = 1$  mM,  $[\text{EDTA}] = 1$  mM, average quantum yield of  $\text{MV}^{+}$  production at 5 mW irradiation ( $\Phi_{\text{MV}^{+}}$ ) = 1.62%).

Analogous photolysis experiments were carried out under acidic conditions at pH 4: no reduction was observed with either the loaded or unloaded samples.

The difference between the high and low pH results can be rationalised with a model for the bio-particles that closely resembles conventional chemical systems. Hence the *K. pneumoniae* CdS particles provide binding sites for methyl viologen that are readily accessible but which are passivated under acidic conditions. In general terms, the mechanism of electron-transfer in the CdS system can be summarised as follows

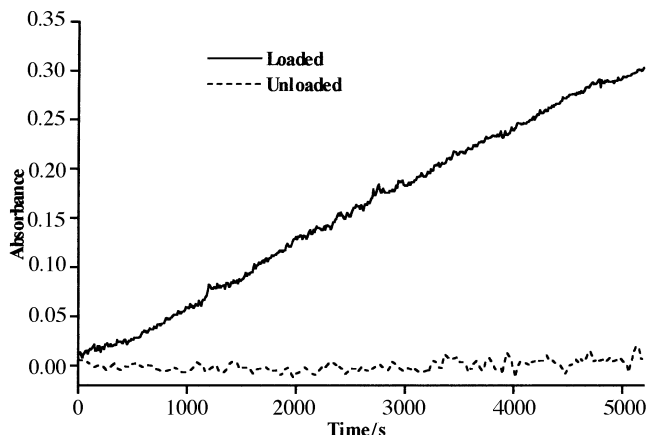
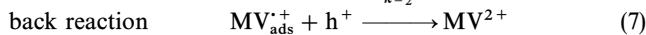
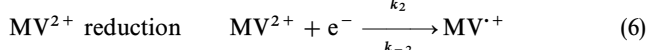
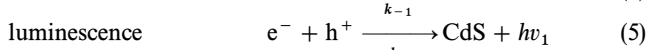
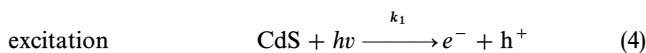


**Fig. 3** Average absorbance values ( $\lambda = 598, 600$  and  $602$  nm) monitored over time, upon irradiation of loaded ( $[\text{CdS}] \approx 0.4$  mM) and unloaded samples of *K. pneumoniae* containing  $\text{MV}^{2+}$  ( $[\text{MV}^{2+}] = 100$   $\mu\text{M}$ ) at pH 10

[reactions (4)–(7)]:<sup>37</sup>



In addition high energy, electrons from the photolysis light source can corrode the semiconductor producing cadmium metal deposits.<sup>2</sup>

The  $\text{MV}^{+}$  radical ion production is in equilibrium with the back reaction whereby it combines with a positive hole in the valence band thus reforming the methyl viologen dication. A net rate of  $\text{MV}^{+}$  accumulation will only be observed if the rate coefficient sequence is in the order  $k_1 > k_{-1}$  and  $k_2 > k_{-2}$ .

The rate of reduction is dependent on two features:<sup>37</sup> (i) the rate of production of the high energy electrons, which will be constant under similar irradiating conditions; (ii) the extent of binding between the particle surface and the redox species.

Using the above model it can be seen why there are differences in photoactivity at high and low pH values for the bio-particles. The positively-charged redox species, methyl viologen, will bind to CdS *via* the surface sulfide,  $\text{S}^{2-}$  sites, which will be more prevalent at pH 10 than in acidic solutions. The behaviour is directly related to the fact that fewer surface  $\text{HS}^-$  sites will be present at low concentrations of hydrogen ions. Furthermore, in acidic conditions hydrogen sulfide can be produced which effectively removes the  $\text{S}^{2-}$  binding sites.

Excess surface  $\text{Cd}^{2+}$  sites will also be more prevalent at lower pH. These not only repel  $\text{MV}^{2+}$  from the semiconductor surface but can also act as radiationless recombination sites thereby using electrons otherwise available for reduction. Under basic conditions  $\text{Cd}^{2+}$  sites will be blocked because they are transformed into cadmium hydroxide,  $\text{Cd}(\text{OH})_2$ , as reported by Spanhel *et al.*<sup>37</sup>

**Methyl orange.** The photoreduction of  $\text{MO}^-$  by CdS particles would be expected to be promoted at different surface sites from  $\text{MV}^{2+}$  because it is a negatively charged species. Measurement of its rate of reduction and comparison with the results obtained using  $\text{MV}^{2+}$  provides a direct method of investigating surface binding to the bio-particles.

Initially, the effect of pH on the rate of photoreduction of methyl orange (20  $\mu\text{M}$ ) was monitored. It has previously been reported that the reduction potential of methyl orange is pH dependent and varies in the following way:  $E^0$  ( $\text{MO}^-/\text{HMO}^-$ ) =  $-0.058$  pH V *vs.* SCE.<sup>29,30,38</sup> The dependency of  $E^0$  on pH is due to the formation of an intermediate semi-reduced radical  $\text{HMO}^-$  which readily reacts to form the hydrazine derivative as described in reactions (2) and (3).

In the present study, at both pH 4 and 10, no photoreduction was observed for unloaded *K. pneumoniae* samples. Measurements of the UV–VIS spectrum at these pH values showed that photolysis of CdS loaded samples ( $[\text{CdS}] \approx 0.4$  mM) produced the reduced protonated form of methyl orange,  $\text{H}_2\text{MO}^-$ . The associated disappearance rates of  $\text{MO}^-$  can be calculated from the absorbance–time profiles shown in Fig. 4(a) and (b): at pH 10 the rate coefficient was  $4.6 \times 10^{-7}$  mol dm<sup>-3</sup> s<sup>-1</sup> whereas at pH 4 the corresponding value was  $1.4 \times 10^{-6}$  mol dm<sup>-3</sup> s<sup>-1</sup>. Therefore a thirty-fold enhancement factor for the photoreduction was measured in acidic solutions. These rates are faster than those obtained by Mills and Green<sup>28</sup> who have reported the rate of methyl orange disappearance for powdered CdS (mean particle diameter > 1  $\mu\text{m}$ ) and colloidal CdS (mean particle diameter = 8 nm). For powdered CdS the rate of disappearance was reported as  $7.7 \times 10^{-8}$  mol dm<sup>-3</sup> s<sup>-1</sup> at pH 4.4 ( $[\text{CdS}] = 10$  mM,

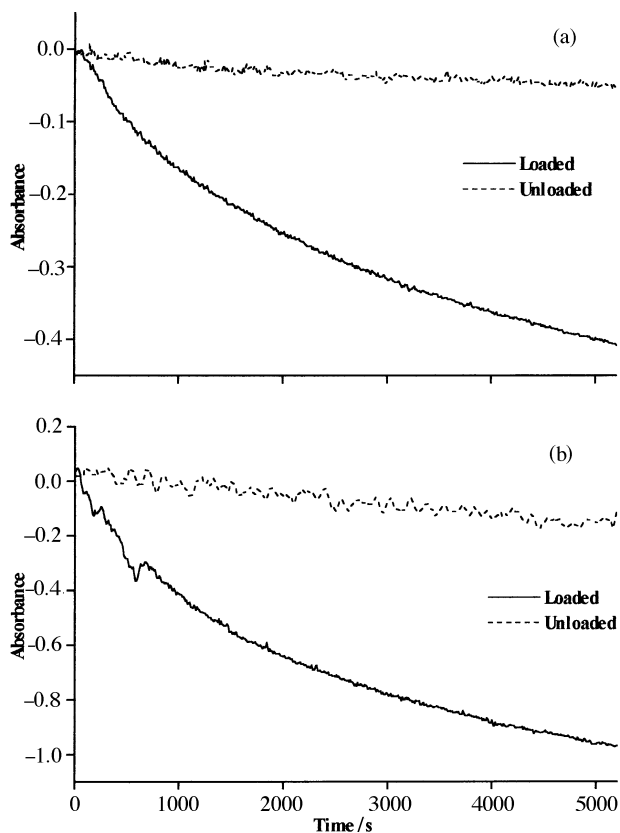


**Fig. 4** (a) Average absorbance values ( $\lambda = 462, 464$  and  $466$  nm) monitored over time, upon irradiation of loaded ( $[\text{CdS}] \approx 0.4$  mM) and unloaded samples of *K. pneumoniae* containing  $\text{MO}^-$  ( $[\text{MO}^-] = 20$   $\mu\text{M}$ ) at pH 10. (b) Average absorbance values ( $\lambda = 462, 464$  and  $466$  nm) monitored over time, upon irradiation of loaded ( $[\text{CdS}] \approx 0.4$  mM) and unloaded samples of *K. pneumoniae* containing  $\text{MO}^-$  ( $[\text{MO}^-] = 0.02$  mM) at pH 4.

( $[\text{MO}^-] = 40$   $\mu\text{M}$ ,  $[\text{EDTA}] = 50$  mM,  $\text{N}_2$  purged solution). As expected the rate of photoreduction of methyl orange by colloidal CdS particles was faster than with the powdered CdS, *i.e.*  $2.7 \times 10^{-7}$  mol  $\text{dm}^{-3}$   $\text{s}^{-1}$  ( $[\text{CdS}] = 0.5$  mM,  $[\text{MO}^-] = 40$   $\mu\text{M}$ ,  $[\text{EDTA}] = 50$  mM,  $\text{N}_2$  purged solution).

The fact that photoreduction of methyl orange occurs is a clear indication that the CdS bio-particles possess photoactive, positively charged surface sites (presumably  $\text{Cd}^{2+}$ ), which promote  $\text{MO}^-$  binding and subsequent electron transfer. This model is confirmed by consideration of the pH effects.

Thus at pH 10 the negatively charged  $\text{S}^{2-}$  surface sites would promote repulsion of the  $\text{MO}^-$  from the bio-particle surface. Furthermore the  $\text{Cd}^{2+}$  sites will be converted into cadmium hydroxide, which has two mechanistic consequences. The first is that incoming  $\text{MO}^-$  ions will not be attracted to these potential redox centres. Secondly, the formation of surface  $\text{Cd}(\text{OH})_2$  will reduce the number of  $\text{Cd}^{2+}$  sites, which could promote radiationless recombination of free electrons. This effect will leave more electrons available for reduction. Overall it should therefore be expected that  $\text{MO}^-$  photoreduction by CdS particles is possible but relatively inefficient at high pH.

From consideration of the pH dependence for the reduction potential of methyl orange discussed above, it can be calculated that at pH 4,  $E^0(\text{MO}^-/\text{HMO}^-) = -0.22$  eV *vs.* SCE compared to  $-0.58$  eV *vs.* SCE at pH 10.<sup>29,30</sup> Although the dependence of the  $E^0$  value for  $\text{MO}^-$  on pH is a source of much debate,<sup>29,30</sup> it does predict that its reduction would be more favourable at the lower pH. However at both pH 10 and 4, the conduction band potential of the semiconductor is considerably more reducing than the reduction potential of  $\text{MO}^-$ .<sup>30</sup> Therefore the effect of pH on the chemical composi-

tion of the bio-particle surface should also be considered.

At acidic pH values,  $\text{S}^{2-}$  surface sites will be transformed into surface  $\text{HS}^-$  ions and possibly  $\text{H}_2\text{S}$ , which may be released into solution. In this situation the approach of  $\text{MO}^-$  to the bio-particle surface will be less restricted by electrostatic repulsion, owing to the reduced negative charge. Furthermore the  $\text{Cd}^{2+}$  surface sites on the CdS particle surface will not be capped by hydroxide groups leading to an increased attraction for the  $\text{MO}^-$ , and subsequent binding. Electron-transfer and photoreduction should increase under these conditions.  $\text{Cd}^{2+}$  radiationless recombination sites will, of course, exist and have a deleterious effect on reduction rate. However, from the results obtained it appears that the effect is small in contrast to the increase in rate caused by the surface attraction.

The results obtained for the bio-particle system are in agreement with those reported for chemically synthesised semiconductor systems. Peral and Mills,<sup>29</sup> using CdS colloids, and Zang *et al.*<sup>30</sup> investigating ZnS sols, observed enhanced rates of reduction of methyl orange at pH 4 compared to pH 10.

**Methyl orange and methyl viologen composite solutions.** It has been reported that the  $\text{MV}^{\cdot+}$  radical ion can re-form the parent  $\text{MV}^{2+}$  ion by passing an electron to another acceptor: this process is termed 'electron relay'.<sup>29,30</sup> For example, in mixed systems of  $\text{MV}^{2+}$  and  $\text{MO}^-$  with colloidal CdS an unexpected enhancement of  $\text{MO}^-$  reduction has been explained in terms of this effect. Therefore as a final probe of the bioparticles' photoredox characteristics, the competitive interaction between  $\text{MV}^{2+}$  and  $\text{MO}^-$  at pH 10 at the bacterial surface was investigated.

CdS loaded and unloaded systems containing  $\text{MO}^-$  (20  $\mu\text{M}$ ),  $\text{MV}^{2+}$  (100  $\mu\text{M}$ ) were prepared. UV-VIS absorption spectra were measured as a function of photolysis time. The absorbance at two wavelengths was monitored: one at 464 nm, which provides a measure of the decrease in  $\text{MO}^-$  concentration and the other at 600 nm for quantification of  $\text{MV}^{\cdot+}$  radical ion production. The addition order of the two reactants to the CdS bio-particles was found, as expected, to have no effect because as determined previously the redox species bind to different surface sites. The kinetic results obtained are shown in Fig. 5. It can be seen that, initially, the methyl orange was reduced, as indicated by the sharp decrease in the absorbance monitored at  $\lambda = 464$  nm, whilst the absorbance at  $\lambda = 600$  nm remained constant. After *ca.* 2000 s the decreasing absorbance at  $\lambda = 464$  nm ceased, the absorbance at  $\lambda = 600$  nm increased rapidly and the solution turned blue

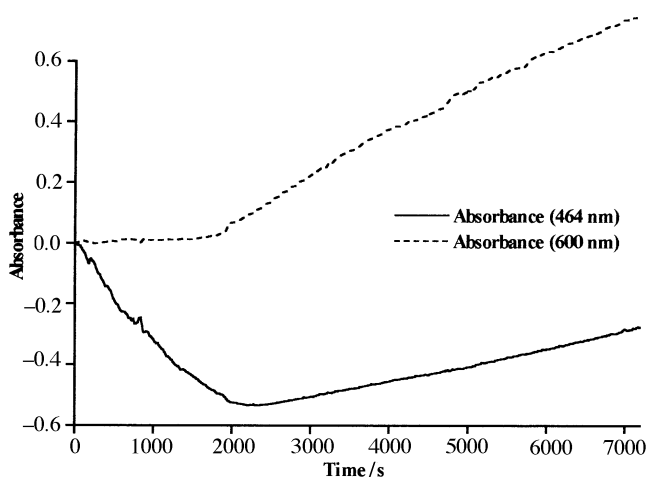


**Fig. 5** Absorbance values ( $\lambda = 464$  and  $600$  nm) monitored over time, upon irradiation of loaded samples ( $[\text{CdS}] \approx 0.4$  mM) of *K. pneumoniae* containing  $\text{MO}^-$  and  $\text{MV}^{2+}$  ( $[\text{MO}^-] = 20$   $\mu\text{M}$ ,  $[\text{MV}^{2+}] = 100$   $\mu\text{M}$ ) at pH 10

indicating the formation of  $MV^{+}$ . Furthermore, after *ca.* 2500 s the absorbance at  $\lambda = 464$  nm, *i.e.*  $MO^{-}$ , was then observed to increase.

No change in either the  $MV^{2+}$  or  $MO^{-}$  signal was observed upon photolysis of unloaded samples.

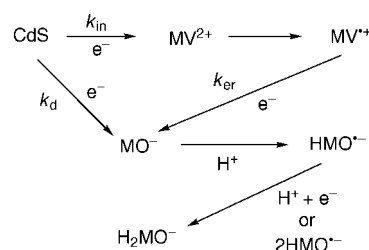
A simple inspection of the individual rate coefficients measured at pH 10 for methyl viologen and methyl orange in this study, *i.e.*  $4.8 \times 10^{-9}$  and  $4.6 \times 10^{-7}$  mol dm<sup>-3</sup> s<sup>-1</sup>, respectively ( $[CdS] \approx 0.4$  mM,  $[MV^{2+}] = 100$   $\mu$ M,  $[MO^{-}] = 20$   $\mu$ M), suggests that  $MO^{-}$  should be reduced preferentially, as compared to  $MV^{2+}$ , in the CdS bio-particle system. Indeed these are the qualitative observations found in the competitive experiments. However the mechanism of interaction between the two species are, as discussed above, quite different and only analysis of the two-component system can provide a quantitative picture of the chemistry.

As seen in Fig. 5 the methyl orange component was observed to be reduced before the methyl viologen with a rate coefficient,  $1.0 \times 10^{-6}$  mol dm<sup>-3</sup> s<sup>-1</sup> ( $[CdS] \approx 0.4$  mM), which is some fifty times faster than in its one-component counterpart. No reduction of  $MV^{2+}$  occurred over the same period of time. Such an observation is, at first sight, surprising because  $MV^{2+}$  was clearly shown to be reduced at pH 10 in its one-component system. This enhancement in reduction rate in the presence of methyl viologen could be due to the  $MV^{2+}$  acting as an electron relay as reported for chemically synthesised semiconductor particles in composite solutions by Peral and Mills<sup>29</sup> and Zang *et al.*,<sup>30</sup> although it may be because of the effect of  $MV^{2+}$  on surface charge. At overpotentials >200 mV, which both  $MO^{-}$  and  $MV^{2+}$  possess, the reduction process is reported to be a diffusion-limited electrochemical reaction.<sup>22</sup> This means that surface characteristics are of great importance, and the reaction could well proceed at a faster rate in the presence of methyl viologen owing to the  $MV^{2+}$  binding to  $S^{2-}$  rich surface sites, and producing a positive electrostatic field around the semiconductor particle.<sup>30</sup> This would allow the  $MO^{-}$  to bind, or come into the close proximity of a greater number of semiconductor particles, and hence cause an increase in electron-transfer and reduction rate.

At pH 10, methyl orange has a reduction potential of *ca.*  $-0.58$  eV *vs.* SCE, compared to a non-pH dependent reduction potential of  $-0.69$  eV for methyl viologen. Under ideal conditions, these data imply that methyl orange would be preferentially photoreduced to methyl viologen with CdS particles. It was not until the methyl orange appeared fully reduced after 2000 s that a blue coloration was observed in the system, and the methyl viologen became reduced at a rate of  $1.0 \times 10^{-8}$  mol dm<sup>-3</sup> s<sup>-1</sup> ( $[CdS] \approx 0.4$  mM), faster than its reduction rate on its own ( $4.8 \times 10^{-9}$  mol dm<sup>-3</sup> s<sup>-1</sup>). The explanation for the increased rate of reduction of methyl viologen in the system containing methyl orange may again be due to the presence of the oppositely charged species making it more electrostatically favourable for binding to the semiconductor surface.

The reason for the preferential reduction of methyl orange over methyl viologen would seem to be simply due to the less negative reduction potential of methyl orange, compared to methyl viologen, at pH 10.

Once the methyl orange becomes fully reduced after 2000 s, the methyl viologen is reduced as indicated by the increase in absorbance observed at 600 nm. The accompanying increase in absorbance at 464 nm could be due to overlap from the absorption band at 600 nm produced by the reduced  $MV^{2+}$ . Additionally, the increase in absorption at 464 nm may be due to the re-formation of the unprotonated  $MO^{-}$ , which absorbs at 464 nm, as the reduced  $H_2MO^{-}$  species becomes oxidised perhaps by substrates in the media. Scheme 1 illustrates the reaction pathways that may be occurring in the illuminated system containing  $MV^{2+}$  and  $MO^{-}$ .



**Scheme 1** Possible electron-transfer scheme for the generation of the radical species  $MV^{\bullet+}$  and  $HMO^{\bullet-}$  (and subsequent  $H_2MO^{\bullet-}$  formation) in the presence of bacterially generated CdS. The methyl orange anionic radical can be formed *via* two pathways; (a) the direct transfer of an electron from the conduction band of CdS ( $k_d$ ) or (b) the indirect transfer of an electron from CdS with  $MV^{2+}$  acting as an 'electron-relay' ( $k_{in} + k_{er}$ ).

## Conclusions

'Bio-CdS' particles synthesised by the bacterium *K. pneumoniae* demonstrate both optical and photoactive traits analogous to chemically synthesised inorganic CdS systems. Optical similarities between the biological and chemical CdS systems are reflected in the luminescence emission spectra obtained for the bio-semiconductor particles; the wavelength of maximum intensity ( $\lambda_{em}$ ) was observed to be close to the onset of absorption ( $\lambda_{onset} \approx 450$  nm) and is possibly excitonic in nature. In colloidal Q-CdS particle systems, excitonic luminescence is frequently noticed upon particle 'activation', achieved under conditions of high pH and in the presence of excess cadmium ions.<sup>31</sup>

The photochemical properties associated with the bio-semiconductor particles establish unequivocally that they have the potential to drive photoinduced reactions presently being undertaken with colloidal CdS dispersions. Both positively charged, *i.e.*  $MV^{2+}$ , and negatively charged species, *i.e.*  $MO^{-}$ , were reduced by the bio-CdS particles at rates comparable to inorganic CdS 'Q-particles'; the rate of reduction of  $MV^{2+}$  by bacterial CdS was similar to that reported by Matsumoto *et al.*<sup>22</sup> for CdS Q-particles with an average diameter of 4.4 nm. This result reflects the non-stoichiometry of the bio-CdS particles under different pH conditions, with  $S^{2-}$  rich sites allowing binding of positively charged species at high pH values and  $Cd^{2+}$  rich surface sites promoting binding of negatively charged species to the semiconductor surface, encouraging electron transfer and hence photoreduction at low pH values. The comparable reduction rate of  $MV^{2+}$  by the bio-CdS and inorganic Q-CdS particles also supports the theory that the large 'superparticles' observed on the bacterial cell wall *ca.* 200 nm in diameter are composed of amorphous discrete quantum dots of CdS approximately 4 nm in diameter.<sup>5,19</sup>

Finally upon examination of the competitive reaction between  $MV^{2+}$  and  $MO^{-}$  the rates of reduction were discovered to be dependent on the surface characteristics of the bio-particles, as seen with their inorganic counterparts. These results coincide with, and give some credence to, the suggestion that in inorganic CdS systems  $MV^{2+}$  can act as an 'electron-relay' transferring electrons to surrounding  $MO^{-}$  molecules.

The authors are grateful to the SERC Biotechnology Directorate/Clean Technology Unit for the award of a research assistantship for P.R.S. and to the Wellcome Trust for the award of a toxicology studentship for J.D.H. Additionally, we would like to thank Professor A.J. Thomson for the use of the UV-VIS spectrometer used in this work.

## References

- 1 J. D. Holmes, P. R. Smith, R. Evans-Gowing, D. J. Richardson, D. A. Russell and J. R. Sodeau, *Arch. Microbiol.*, 1995, **163**, 143.

- 2 J. D. Holmes, P. R. Smith, R. Evans-Gowing, D. J. Richardson, D. A. Russell and J. R. Sodeau, *Photochem. Photobiol.*, 1995, **62**, 1022.
- 3 H. Aiking, K. Kok, H. van Heerikhuizen and J. van't Riet, *Appl. Environ. Microbiol.*, 1982, **44**, 938.
- 4 H. Aiking, A. Stijnman, C. van Garderen, H. van Heerikhuizen and J. van't Riet, *Appl. Environ. Microbiol.*, 1984, **47**, 374.
- 5 J. D. Holmes, D. J. Richardson, S. Saed, R. Evans-Gowing, D. A. Russell and J. R. Sodeau, *Microbiology*, 1997, **143**, 2521.
- 6 G. Z. Jaeckel, *Tech. Phys.*, 1926, **7**, 301.
- 7 J. K. Inman, A. M. Mraz and W. A. Weyl, *Solid Luminescent Materials*, Wiley, New York, 1st edn., 1948, p. 182.
- 8 R. Rossetti, S. Nakahara and L. E. Brus, *J. Chem. Phys.*, 1983, **79**, 1086.
- 9 R. Rossetti, J. L. Ellison, J. M. Gibson and L. E. Brus, *J. Chem. Phys.*, 1984, **80**, 4464.
- 10 R. N. Reese, R. K. Mehra, E. B. Tarbet and D. R. Winge, *J. Biol. Chem.*, 1988, **263**, 4186.
- 11 R. N. Reese and D. R. Winge, *J. Biol. Chem.*, 1988, **263**, 12832.
- 12 C. T. Dameron, B. R. Smith and D. R. Winge, *J. Biol. Chem.*, 1989, **264**, 17355.
- 13 R. K. Mehra, P. Mulchindani and T. C. Hunter, *Biochem. Biophys. Res. Commun.*, 1994, **200**, 1193.
- 14 C. T. Dameron, R. N. Reese, R. K. Mehra, A. R. Kortan, P. J. Carroll, M. L. Steigerwald, L. E. Brus and D. R. Winge, *Nature (London)*, 1989, **338**, 596.
- 15 J. Barbas, V. Santhanagopalan, M. Blaszczyński, W. R. Ellis Jr and D. R. Winge, *J. Inorg. Biochem.*, 1992, **48**, 95.
- 16 C. T. Dameron and D. R. Winge, *Inorg. Chem.*, 1990, **29**, 1343.
- 17 E. Grill, E. L. Winnacker and M. H. Zenk, *FEBS*, 1986, **197**, 115.
- 18 R. K. Mehra, E. B. Tarbet, W. R. Gray and D. R. Winge, *Proc. Natl. Acad. Sci. USA*, 1988, **85**, 8815.
- 19 J. D. Holmes, J. A. Farrar, D. J. Richardson, D. A. Russell and J. R. Sodeau, *Photochem. Photobiol.*, 1997, **65**, 811.
- 20 A. Henglein, *J. Chim. Phys.*, 1987, **84**, 1043.
- 21 S. Ogawa, F. F. Fan and A. J. Bard, *J. Phys. Chem.*, 1995, **99**, 11182.
- 22 H. Matsumoto, H. Uchida, T. Matsunaga, K. Tanaka, T. Sakata, H. Mori and H. Yoneyama, *J. Phys. Chem.*, 1994, **98**, 11549.
- 23 Y. Nosaka and M. A. Fox, *Langmuir*, 1987, **3**, 1147.
- 24 K. Komers, *J. Chem. Res. (S)*, 1994, 293.
- 25 J. W. Park, J. H. Kim, B. K. Hwang and K. Park, *Chem. Lett.*, 1994, 2075.
- 26 G. T. Brown and J. R. Darwent, *J. Phys. Chem.*, 1984, **88**, 4955.
- 27 A. Mills and G. Williams, *J. Chem. Soc., Faraday Trans. 1*, 1987, **83**, 2647.
- 28 A. Mills and A. Green, *J. Photochem. Photobiol. A: Chem.*, 1991, **59**, 199.
- 29 J. Peral and A. Mills, *J. Photochem. Photobiol. A: Chem.*, 1993, **73**, 47.
- 30 L. Zang, C. Y. Liu and X. M. Ren, *J. Photochem. Photobiol. A: Chem.*, 1995, **85**, 239.
- 31 H. Weller, *Angew. Chem., Int. Ed. Engl.*, 1993, **32**, 41.
- 32 W. A. Pickett and A. C. R. Dean, *Microbios*, 1976, **15**, 79.
- 33 B. Kierdaszuk, I. Gryczynski, A. Modrak-Wojcik, A. Bzowska, D. Shugar and J. R. Lakowicz, *Photochem. Photobiol.*, 1995, **61**, 319.
- 34 A. J. Hoffman, G. Mills, H. Yee and M. R. Hoffmann, *J. Phys. Chem.*, 1992, **96**, 5546.
- 35 T. Uchihara, M. Matsumara, J. Ono and H. Tsubomura, *J. Phys. Chem.*, 1990, **94**, 415.
- 36 T. Uchihara, T. Nakamura and A. Kinjo, *J. Photochem. Photobiol. A: Chem.*, 1992, **66**, 379.
- 37 L. Spanhel, M. Haase, H. Weller and A. Henglein, *J. Am. Chem. Soc.*, 1987, **109**, 5649.
- 38 A. Mills and G. Williams, *J. Chem. Soc., Faraday Trans. 1*, 1989, **85**, 503.

Paper 7/08742J; Received 4th December, 1997